

Microscopic phase-field simulation of ordered domain interfaces formed between DO₂₂ phases along [100] direction

ZHANG Ming-yi(张明义)¹, CHEN Zheng(陈 铮)^{1,2}, WANG Yong-xin(王永欣)¹,
LU Yan-li(卢艳丽)¹, ZHANG Li-peng(张利鹏)¹, ZHAO Yan(赵 彦)¹

1. School of Materials Science and Engineering, Northwestern Polytechnical University, Xi'an 710072, China;
2. State Key Laboratory of Solidification Processing, Northwestern Polytechnical University, Xi'an 710072, China

Received 23 September 2008; accepted 9 January 2009

Abstract: Ordered domain interfaces formed between DO₂₂ (Ni₃V) phases along [100] direction during the precipitation process of Ni₇₅Al_xV_{25-x} alloys were simulated by using the microscopic phase-field model. The atomic structure, migration process, and compositions of interfaces were investigated. It is found that there are four kinds of stable ordered domain interfaces formed between DO₂₂ phases along [100] direction and all of them can migrate. During the migration of interfaces, the jump of atoms shows site selectivity behaviors and each stable interface forms a distinctive transition interface. The atom jump selects the optimistic way to induce the migration of interface, and the atomic structures of interfaces retain the same before and after the migration. The alloy elements have different preferences of segregation or depletion at different interfaces. At all the four kinds of interfaces, Ni and Al segregate but V depletes. The degrees of segregation and depletion are also different at different interfaces.

Key words: interface migration; solute segregation; site selectivity; microscopic phase-field; ordered domain interface

1 Introduction

The behavior of interfaces and microstructure evolution are interdependent, as observed during fundamental annealing phenomena such as grain growth and recrystallization. The physical and chemical properties of a bulk material may be modified or changed significantly in the presence of interface[1]. For example, altering the distribution of boundary types in bulk metals via thermal mechanical processing can lead to significant improvement in material performances[2–3]. Most types of thermal mechanical processing (e.g., annealing, hot rolling, extrusion, forging, super plastic deformation, recrystallization and grain growth) modify the grain structure and the distribution of interfaces. It is important to understand the interface property in the thermal mechanical processing process. One key for predicting the effects of these types of processing methods on materials properties is to understand how interfaces

move. This remains one of the longest standing, yet least understood problems in physical metallurgy.

Atomistic simulation has been one of the most powerful methods for exploring many aspects of the solid interface behaviors today, especially in the area that experiment techniques are still problematic to investigate, such as the connection among atomic interface structure, interface dynamics and interface migration[4–8]. Molecular Dynamics and Monte Carlo method has been the useful atomistic methods of choice for observing dynamical effects, such as grain boundary migration, on the microstructure evolution. GONG and LIU[9] studied the solid state amorphization in immiscible Cu-Ta system using the Molecular Dynamics method, and it is found that the interface structure affects the stability of interfaces and the asymmetrical growth of the amorphous phases. The energies and mobilities of interfaces on the evolution of the microstructure had been studied by using the Molecular Dynamics and Monte Carlo method [10]. Previous study demonstrated that the interface

Foundation item: Projects(50671084, 50875217) supported by the National Natural Science Foundation of China; Projects(2003E106, SJ08-ZT05) supported by the Natural Science Foundation of Shaanxi Province, China; Project(20070420218) supported by China Postdoctoral Science Foundation

Corresponding author: ZHANG Ming-yi; Tel: +86-29-88474095; E-mail: zmy1688@gmail.com
DOI: 10.1016/S1003-6326(08)60334-9

mobility is strongly dependent on misorientation[11] and interface structure[12]. Recently, an atomistic simulation technique, the microscopic phase-field model, has been used to study the migration characteristic of interfaces during the precipitation process of nickel based alloys. It is found that this method can study not only the microstructure evolution but also the atomic behavior of interface migration[13].

In the present work, we investigated the atomic structure, migration process, and compositions of ordered domain interfaces formed between DO₂₂ phases along [100] direction during the precipitation process of Ni₇₅Al_xV_{25-x} alloys using the microscopic phase-field model.

2 Microscopic phase-field model

Microscopic phase-field model, based on the microscopic diffusion equations that are the discrete lattice form of the Cahn-Hilliard equations, was first proposed by KHACHATURYAN[14] and developed by PODURI and CHEN[15] for the ternary alloy system. The equations for ternary alloy systems read as

$$\left\{ \begin{aligned} \frac{dP_A(r,t)}{dt} &= \frac{1}{k_B T} \sum_{r'} \left[L_{AA}(r-r') \frac{\partial F}{\partial P_A(r',t)} + \right. \\ &\quad \left. L_{AB}(r-r') \frac{\partial F}{\partial P_B(r',t)} \right] \\ \frac{dP_B(r,t)}{dt} &= \frac{1}{k_B T} \sum_{r'} \left[L_{BA}(r-r') \frac{\partial F}{\partial P_A(r',t)} + \right. \\ &\quad \left. L_{BB}(r-r') \frac{\partial F}{\partial P_B(r',t)} \right] \end{aligned} \right. \quad (1)$$

For ternary systems, $P_C(r,t) = 1 - P_A(r,t) - P_B(r,t)$, where $P_\alpha(r,t)$ ($\alpha = A, B$ or C) represents the probabilities

of finding an atom α at a given lattice site r at a given time t which is a reduced time; $L_{\alpha\beta}(r-r')$ (α and $\beta = A, B$ or C) is the kinetic coefficient proportional to the probabilities of elementary diffusional jumps from site r to r' per unit of time; and F is the total Helmholtz free energy of the system based on the mean-field approximation, which can be written as a function of single site occupation probability:

$$F = -\frac{1}{2} \sum_r \sum_{r'} [V_{AB}(r-r')P_A(r)P_B(r') + V_{BC}(r-r')P_B(r)P_C(r') + V_{AC}(r-r')P_A(r)P_C(r')] + k_B T \sum_r [P_A(r)\ln P_A(r) + P_B(r)\ln P_B(r) + P_C(r)\ln P_C(r)] \quad (2)$$

where the effective pair interaction $V_{\alpha\beta}$ is deduced from the pair interaction, $\omega_{\alpha\beta}: V_{\alpha\beta} = \omega_{\alpha\alpha} + \omega_{\beta\beta} - 2\omega_{\alpha\beta}$.

For the convenience of analysis and visualization of the atomic configuration and multiphase morphologies, and considering the proper time consumption, our numerical simulation are carried out in a 2D square super-cell consisting of 128×128 square lattice sites by the projection of 3D crystal structure of Ni₃V (DO₂₂) along [010] direction. Schematic diagrams of the DO₂₂ crystal structure of Ni₃V and the projection of DO₂₂ (Ni₃V) structure along [010] direction are shown in Figs.1(a) and (b), respectively. Eq.(1) is solved in the reciprocal space using the Modified Euler’s method with the time increment equal to 0.000 2. The real-space atomic site occupation probability of alloying elements is obtained by the Back-Fourier transformation of the solution of Eq.(1).

With the atomic pair interactions as the only inputs and without any prior assumption concerning the atomic structure of ordered phases, the model can describe the

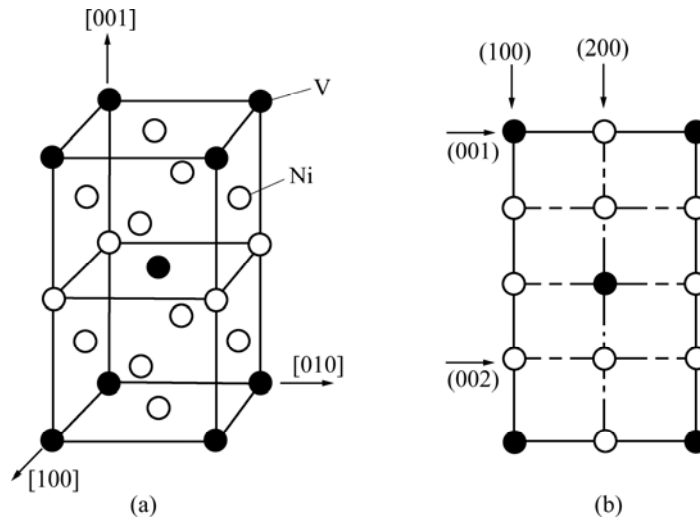


Fig.1 Schematic diagrams of crystal structure of DO₂₂ (a) and its projection along [010] direction (b)

ordering, phase separation, growth and coarsening process of ordered phases simultaneously within the same formalism, and can produce crystallographic structures of various possible ordered phases and atomic configurations by minimizing the total energy of the alloy system. The applications of microscopic phase-field model in the studies of the phase transformation and coarsening process of ordered phases in binary and ternary alloy systems have shown excellent agreement both with experiment results and other simulation results[16–17].

3 Results and discussion

3.1 Atomic structure and migration of interfaces

Fig.2 shows the atomic microstructure evolution of $\text{Ni}_{75}\text{Al}_3\text{V}_{22}$ alloy aged at 1 150 K. Fig.3 shows the atomic microstructure evolution of $\text{Ni}_{75}\text{Al}_{4.2}\text{V}_{20.8}$ alloy aged at 1 200 K. In the simulated picture, the black sites represent the Ni, which seems to form a background color. The gray sites represent the V. When the site occupation probability of V is low, the V sites would

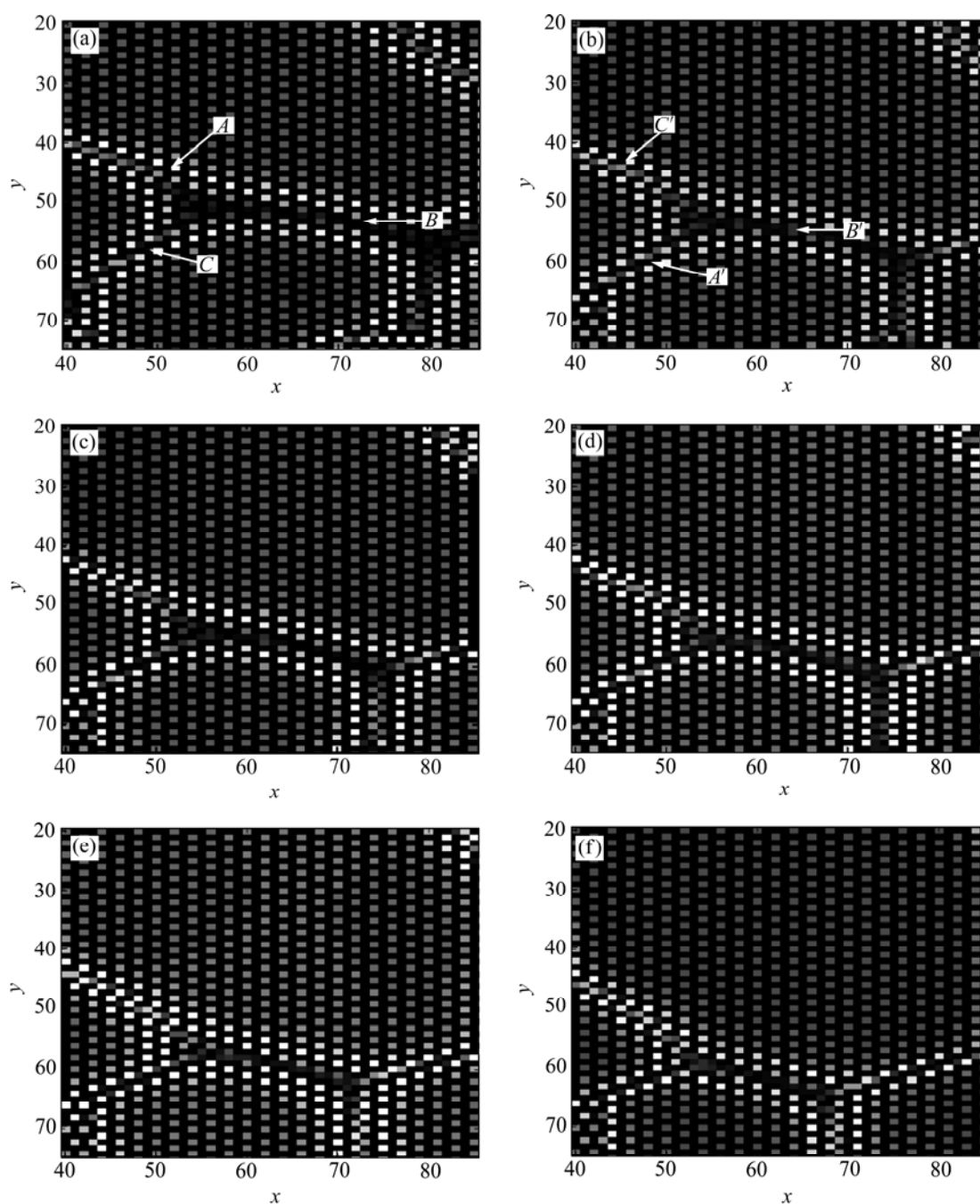


Fig.2 Atomic microstructure evolution pictures of $\text{Ni}_{75}\text{Al}_3\text{V}_{22}$ alloy aged at 1 150 K: (a) $t=1.1 \times 10^5$; (b) $t=2.0 \times 10^5$; (c) $t=2.3 \times 10^5$; (d) $t=2.6 \times 10^5$; (e) $t=3.0 \times 10^5$; (f) $t=4.0 \times 10^5$

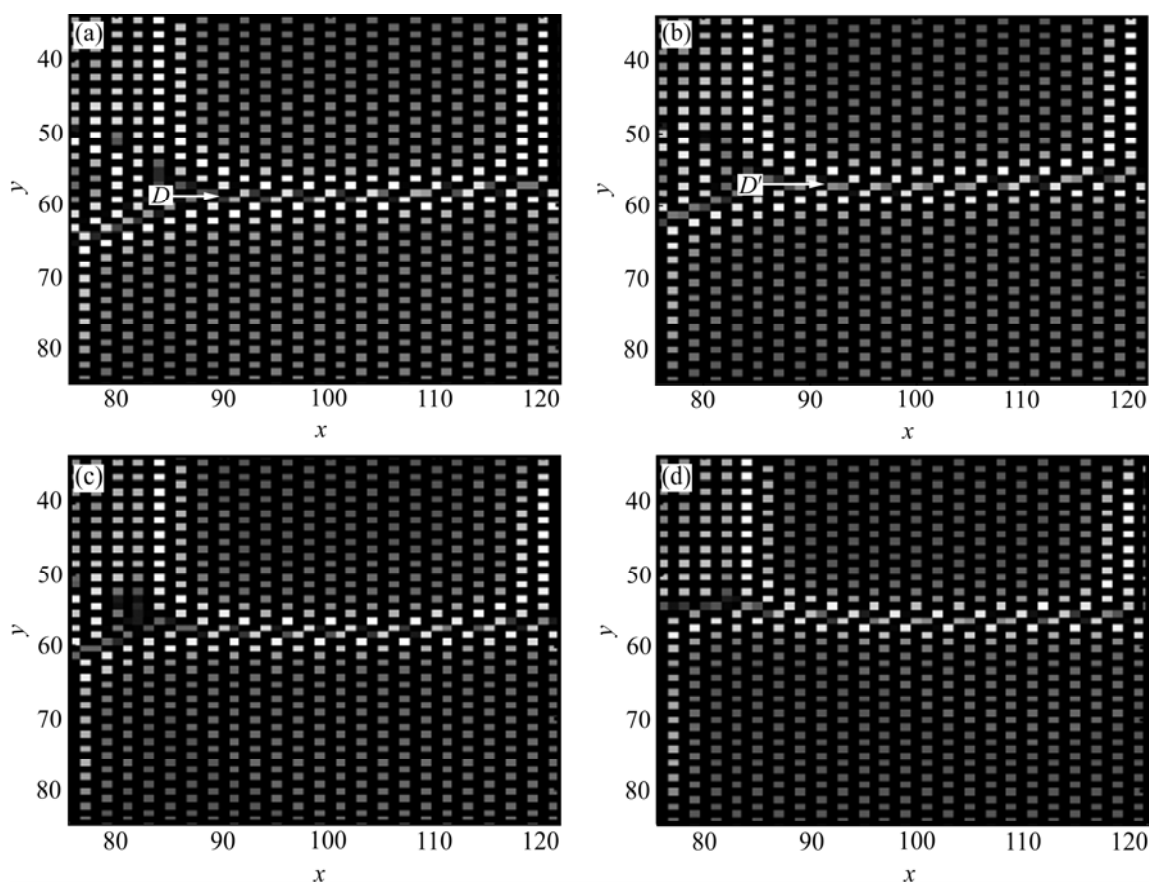


Fig.3 Atomic microstructure evolution pictures of $\text{Ni}_{75}\text{Al}_{4.2}\text{V}_{20.8}$ alloy aged at 1 200 K: (a) $t=3.0 \times 10^5$; (b) $t=3.2 \times 10^5$; (c) $t=3.4 \times 10^5$; (d) $t=4.0 \times 10^5$

become bright, such as the sites near the interfaces.

By analyzing the atomic arrangement of interface using the atomic microstructure evolution picture, and combination with the site occupation probability of alloy elements on the site of interfaces, the atomic structure of these interfaces of DO_{22} phases along $[100]$ direction are identified. They are interface $\{102\} \cdot 1/2[00\bar{1}]$ denoted by arrow A in Fig.2(a), interface $\{102\} \cdot 1/2[100]$ denoted by arrow B in Fig.2(a), interface $\{102\} \cdot 1/2[001]$ denoted by arrow C in Fig.2(a), and interface $\{100\} \cdot 1/2[00\bar{1}]$ denoted by arrow D in Fig.3(a). Figs.4(a)–(d) show the schematic diagrams of the atomic structure of interface $\{102\} \cdot 1/2[00\bar{1}]$, $\{102\} \cdot 1/2[100]$, $\{102\} \cdot 1/2[001]$ and $\{100\} \cdot 1/2[00\bar{1}]$, respectively. As Fig.2 and Fig.3 show, all the studied interfaces migrate in the process of microstructure evolution. The interfaces formed in the process of migration are also identified. In the present work, the interfaces formed in the process of migration are named as transition interfaces, and the original interfaces before and after the migration are named as stable interfaces.

By analyzing the atom jump mode of interfaces during the migration, it is found that each kind of stable interface forms only one kind of transition interface, for the atom jump shows a site selectivity behavior in the

process of migration. The interfaces denoted by arrow A' – C' in Fig.2(b) and D' in Fig.3(b) are the transition interfaces of stable interface $\{102\} \cdot 1/2[00\bar{1}]$, $\{102\} \cdot 1/2[100]$, $\{102\} \cdot 1/2[001]$ and $\{100\} \cdot 1/2[00\bar{1}]$, respectively, and Figs.4(e)–(h) show the schematic diagrams of the structure of transition interfaces denoted by arrow A' – D' . For the convenience of discussion, numbers 1–8 are labeled at the site of stable interfaces.

According to the simulated atomic microstructure evolution pictures, the V atoms on the sites labeled by No.1 exchange with the Ni at the sites labeled by No.2 during the migration process of interface $\{102\} \cdot 1/2[00\bar{1}]$; and the V atoms migrate along $[100]$ direction (perpendicular to the interface). While the V atoms at the sites labeled by No.3 exchange with the Ni at the sites labeled by No.4 during the migration process of interface $\{102\} \cdot 1/2[100]$. The V atoms at the sites labeled by No.5 exchange with the Ni at the sites labeled by No.6 during the migration process of interface $\{102\} \cdot 1/2[001]$. The V atoms at the sites labeled by No.7 exchange with the Ni at the sites labeled by No.8 during the migration process of interface $\{100\} \cdot 1/2[00\bar{1}]$. In these three kinds of interfaces, the V atoms migrate along $[001]$ direction (parallel to the interface) during the migration process.

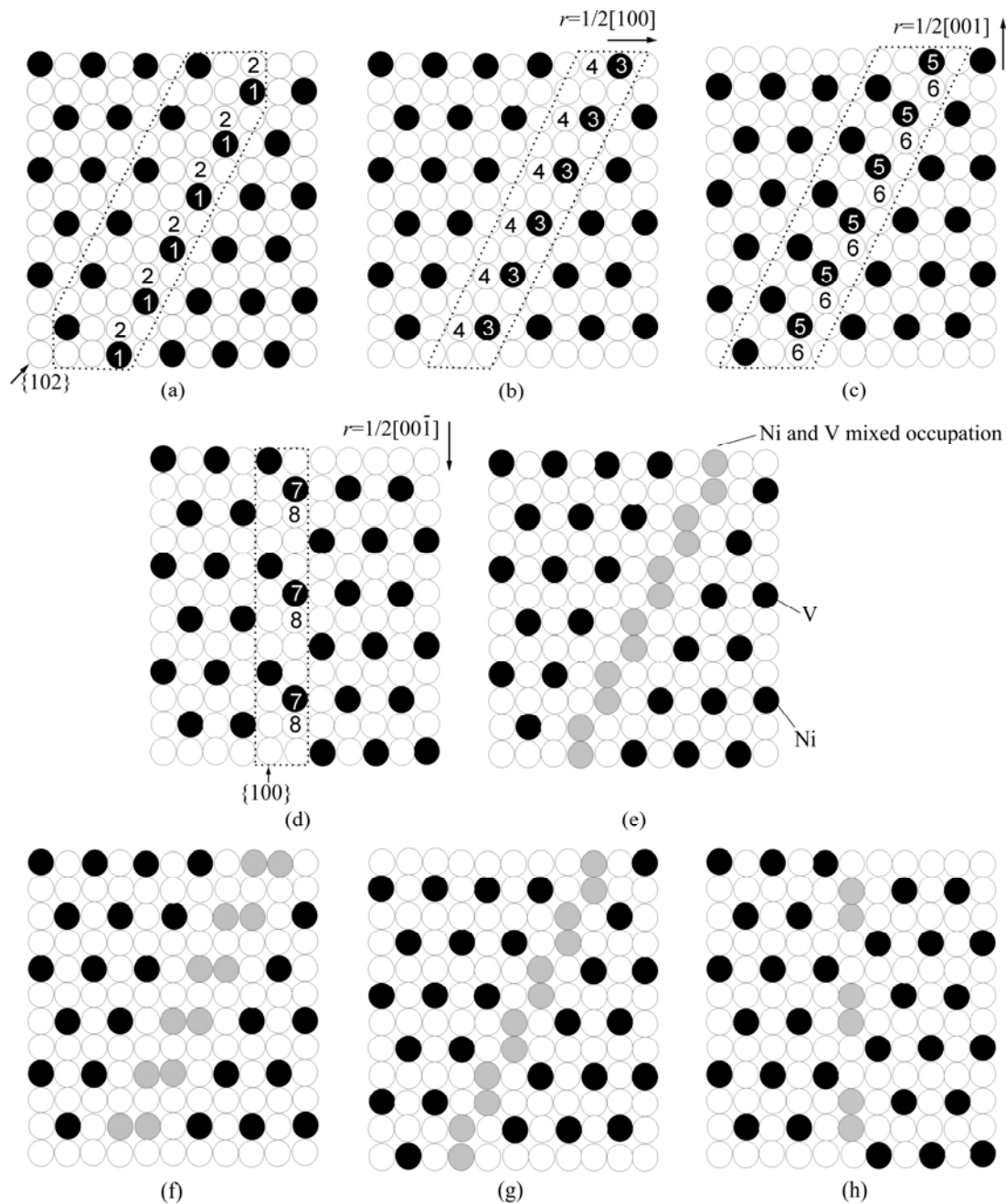


Fig.4 Schematic diagrams of atomic structure of interfaces: (a) $\{102\} \cdot 1/2[00\bar{1}]$; (b) $\{102\} \cdot 1/2[100]$; (c) $\{102\} \cdot 1/2[001]$; (d) $\{100\} \cdot 1/2[00\bar{1}]$; (e)–(h) Transition interfaces formed in migration process of stable interfaces (a)–(d), respectively

To verify the atom jump mode of each interface, the site occupation probability evolution of Ni and V at the site labeled by 1–8 is shown in Fig.5. Fig.5(a) shows the site occupation probability evolution of Ni and V at the sites 1 and 2. The site occupation probability of V at the site 1 decreases while the site occupation probability of V at the site 2 increases. The site occupation probability of V at the sites 1 or 2 shows symmetrical but contrary evolution, the same as the site occupation probability evolution of Ni. At the site 1 or site 2, the site occupation probability of V and Ni also shows symmetrical but contrary evolution. Then it can be concluded that, during

the migration of interface $\{102\} \cdot 1/2[100]$, the V atoms at sites 1 jump to the nearest sites labeled by No.2; and at the same time, the Ni atoms at site 2 jump to the nearest sites labeled by No.1. It is the exchange of the V at the site 1 and the Ni at the site 2 that make the interface $\{102\} \cdot 1/2[00\bar{1}]$ migrate. It also can be seen that after the exchange of the Ni and V atoms, the atomic structure of interface $\{102\} \cdot 1/2[00\bar{1}]$ remains the same.

According to Figs.5(b), (c) and (d), it can be concluded that the V at the site 3 exchanges with the Ni at the site 4 during the migration process of interface $\{102\} \cdot 1/2[100]$; the V at the site 5 exchanges with the Ni

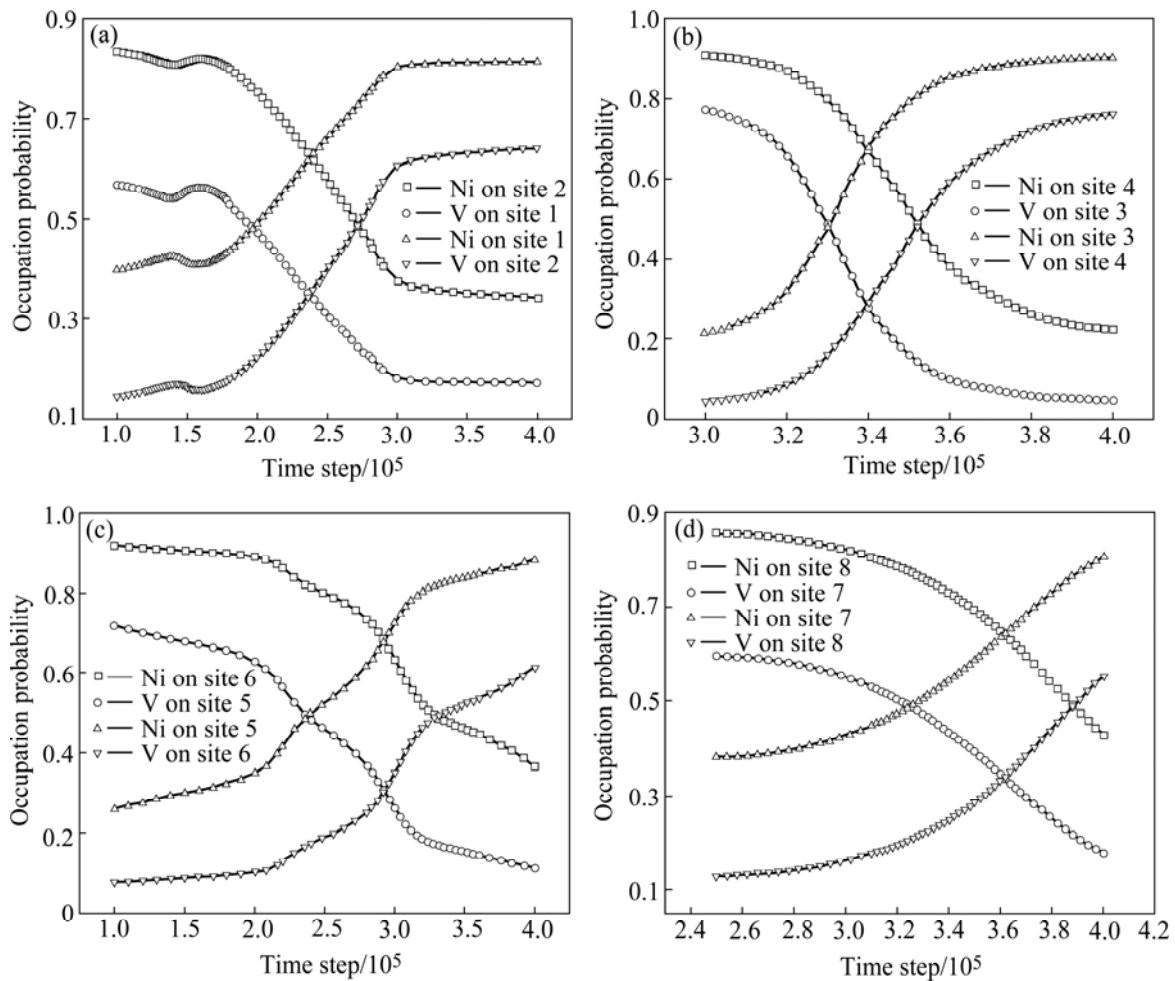


Fig.5 Occupation probabilities evolution of V and Ni at sites 1–8 at interfaces

at the site 6 during the migration process of interface $\{102\} \cdot 1/2[00\bar{1}]$; and the V at the site 7 exchanges with the Ni at the site 8 during the migration process of interface $\{100\} \cdot 1/2[00\bar{1}]$. It should be noticed that the atomic structures of all the studied interfaces remain the same before and after the migration. Then, it is easy to understand that it is the site selectivity behavior of atoms that force the atomic structures of interfaces retain the same before and after the migration. It can also be found that, among all the possible atomic jump modes it may induce the migration of interfaces, and the number of atoms that need to jump during the migration is the least. That is to say, the atom jump mode to induce the migration of interfaces is the way of the least resistance. In other words, the atom jumps select the optimistic way in the aspect of kinetics and thermodynamics to induce the migration of interfaces.

3.2 Solute segregation and depletion of interfaces

The composition distributions of alloy elements, represented by the average site occupation probabilities of alloy elements, across the interfaces were calculated

as shown in Fig.6. The compositions of interfaces $\{102\} \cdot 1/2[00\bar{1}]$, $\{102\} \cdot 1/2[100]$, and $\{102\} \cdot 1/2[001]$ were calculated at the time step of 2.0×10^5 , and $\{100\} \cdot 1/2[00\bar{1}]$ was calculated at the time step of 4.0×10^5 . The compositions of alloy elements at the interfaces are different from that inside the domains. The compositions of interfaces are related to the atomic structure of interfaces. At all the four kinds of studied interfaces, Ni and Al segregate but V depletes. The degrees of segregation and depletion of alloy elements are different at different interfaces. At the interface $\{102\} \cdot 1/2[100]$, the concentration of Ni or Al is the highest and the composition of V is the lowest among the four kinds of studied interfaces. The composition of Al or Ni at the interface $\{100\} \cdot 1/2[00\bar{1}]$ is the lowest, and the composition of V at the interface $\{100\} \cdot 1/2[00\bar{1}]$ is the highest among the four kinds of studied interfaces. Analyzing the atomic structure of the four kinds of interfaces, it can be found that there is no Ni atom plain at the interface $\{100\} \cdot 1/2[00\bar{1}]$, while there are two Ni atom plains at the interface $\{102\} \cdot 1/2[100]$. Then, it is reasonable that the concentration of Ni is the highest and

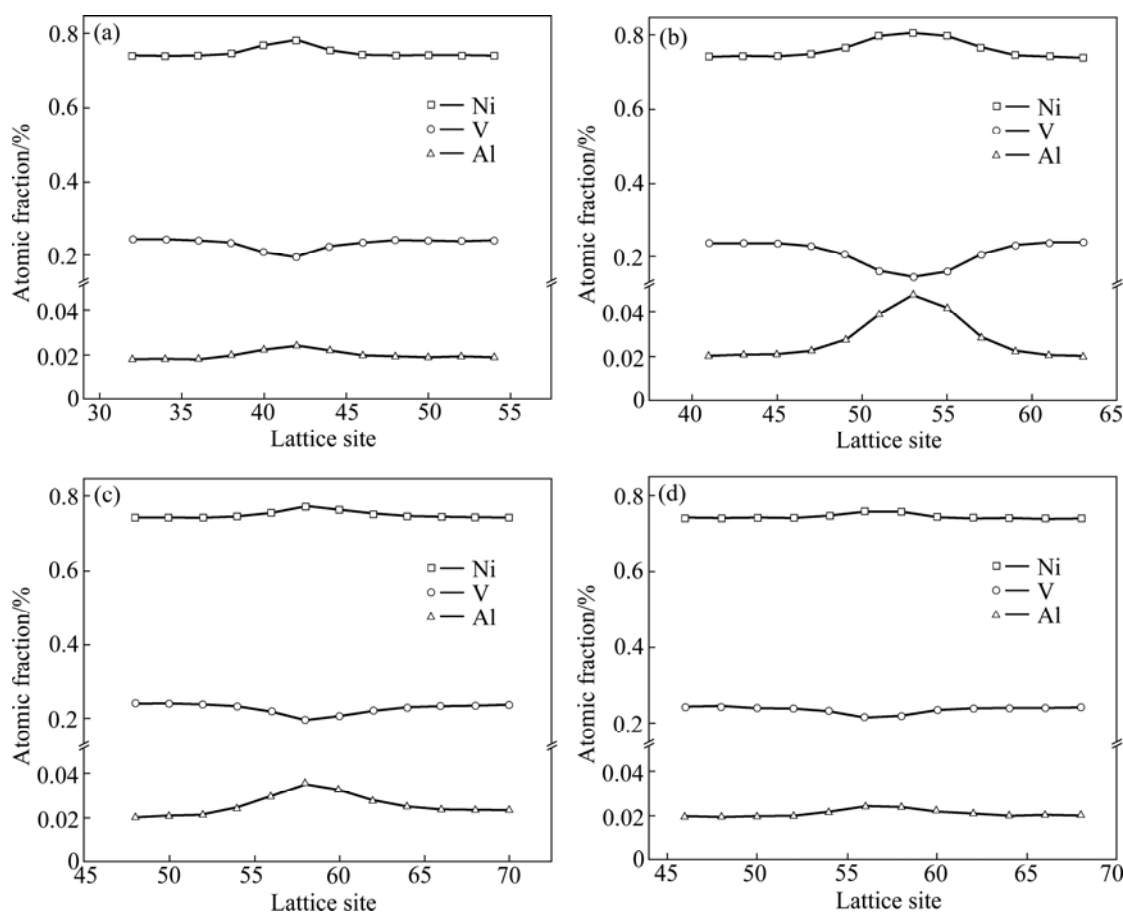


Fig.6 Composition distribution of alloy elements across interfaces: (a) $\{102\} \cdot 1/2[00\bar{1}]$ at time step of 2.0×10^5 ; (b) $\{102\} \cdot 1/2[100]$ at time step of 2.0×10^5 ; (c) $\{102\} \cdot 1/2[001]$ at time step of 2.0×10^5 ; (d) $\{100\} \cdot 1/2[00\bar{1}]$ at time step of 4.0×10^5

the concentration of V is lowest at interface $\{102\} \cdot 1/2[100]$; the concentration of Ni is the lowest and the concentration of V is the highest at interface $\{100\} \cdot 1/2[00\bar{1}]$. The segregation of alloy element is related to the site preference behavior[18]. Further studies will be carried out to study the site preference behavior of Al at the site of interfaces.

4 Conclusions

1) There are four kinds of stable interfaces formed between DO_{22} phases along $[100]$ direction and all of them can migrate. During the migration, each of them forms one kind of transition interface.

2) The atoms show site selective behavior during the migration of interfaces and site selectivity behavior of atoms forces the atomic structures of interfaces retain the same before and after the migration. The atom jump modes are the optimum way to induce the migration of interfaces.

3) The elements of alloy have different preferences of segregation or depletion at different interfaces. At all the studied interfaces, Ni and Al segregate and V depletes.

4) The degrees of segregation and depletion are also different at different interfaces. At the interface $\{102\} \cdot 1/2[100]$, the concentration of Ni or Al is the highest and the composition of V is the lowest, while at the interface $\{100\} \cdot 1/2[00\bar{1}]$, the concentration of Ni or Al is the lowest and the composition of V is the highest among the four kinds of studied interfaces.

References

- [1] WANG S Q, YE H Q. Theoretical studies of solid-solid interfaces [J]. *Curr Opin Solid State Mater Sci*, 2006, 10(1): 26–32.
- [2] RABKIN E, AMOUYAL Y, KLINGER L. Scanning probe microscopy study of grain boundary migration in NiAl [J]. *Acta Mater*, 2004, 52: 4953–4959.
- [3] SAKATA T, YASUDA H Y, UMAKOSH Y. Interphase boundary fracture and grain boundary precipitation of $Ni_3Al(\gamma)$ phase in β -NiAl bicrystals [J]. *Acta Mater*, 2003, 51(6): 1561–1572.
- [4] BOS C, SOMMER F, MITTEMEIJER E J. An atomistic analysis of the interface mobility in a massive transformation [J]. *Acta Mater* 2005, 53(20): 5333–5341.
- [5] ZHANG H, MENDELEV M I, SROLOVITZ D J. Computer simulation of the elastically driven migration of a flat grain boundary [J]. *Acta Mater* 2004, 52(9): 2569–2576.
- [6] OGUMA R, EGUCHI T, MATSUMURA S, SON S K. Domain growth and off-phase boundary structures in $L1_2$ -type ordering [J].

- Acta Mater, 2006, 54(6): 1533–1539.
- [7] HOWE J M, GAUTAM A R S, CHATTERJEE K, PHILLIP F. Atomic-level dynamic behavior of a diffuse interphase boundary in an Au-Cu alloy [J]. Acta Mater, 2007, 55(6): 2159–2171.
- [8] LOJKOWSKI W, FECHT H. The structure of intercrystalline interfaces [J]. Prog Mater Sci, 2000, 45(5/6): 339–568.
- [9] GONG H R, LIU B X. Influence of interfacial texture on solid-state amorphization and associated asymmetric growth in immiscible Cu-Ta multilayers [J]. Physical Review B, 2004, 70(10): 134202–134209.
- [10] UPMANYU M, HASSOLD G N, KAZARYAN A, HOLM E A, WANG Y, PATTON B, SROLOVITZ D J. Boundary mobility and energy anisotropy effects on microstructural evolution during grain growth [J]. Interface Sci, 2002, 10(2): 201–216.
- [11] GOTTSTEIN G, MOLODOV D A, SHIVINDLERMAN L S, SROLOVITZ D J, WINNING M. Grain boundary migration: Misorientation dependence [J]. Curr Opin Solid State Mater Sci, 2001, 5(1): 9–14.
- [12] ZHANG Ming-yi, WANG Yong-xin, CHEN Zheng, ZHANG Jing, ZHAO Yan, ZHEN Hui-hui. Simulation of ordered domain interfaces formed between $L1_2$ phases in Ni-Al-V alloy using microscopic phase-field model [J]. Acta Metallurgica Sinica, 2007, 43(10): 1101–1106. (in Chinese)
- [13] LI Y S, CHEN Z, LU Y L, WANG Y X, LAI Q B. Microscopic phase-field simulation of atomic migration characteristics in $Ni_{75}Al_xV_{25-x}$ alloys [J]. Mater Lett, 2007, 61: 974–978.
- [14] KHACHATURYAN A G. Theory of structural transformations in solids [M]. New York: Wiley, 1983: 23–26.
- [15] PODURI R, CHEN L Q. Computer simulation of atomic ordering and compositional clustering in the pseudobinary Ni_3Al-Ni_3V system [J]. Acta Mater, 1998, 46(5): 1719–1729.
- [16] PAREIGE C, BLAVATTE D. Simulation of the FCC-FCC+ $L1_2$ + DO_{22} kinetic reaction [J]. Scripta Mater, 2001, 44(2): 243–247.
- [17] LU Y L, CHEN Z, WANG Y X. Microscopic phase-field simulation of the early precipitation mechanism of Ni_3Al phase in Ni-Al alloys [J]. Mater Lett, 2008, 62(8/9): 1385–1388.
- [18] KITASHIMA T, YOKOKAWA T, YEH A C, HARADA H. Analysis of element content effects on equilibrium segregation at γ/γ' interface in Ni-based superalloys using the cluster variation method [J]. Intermetallics, 2008, 16(6): 779–784.

(Edited by YANG Hua)